BIOCHEMISTRY
including biophysical chemistry & molecular biology
Article

Biochemistry **2010,** *49,* 3317–3326 3317
DOI: 10.1021/bi901962p

Insights into the Specificity of Thioredoxin Reductase−Thioredoxin Interactions. A Structural and Functional Investigation of the Yeast Thioredoxin System[†]

Marcos A. Oliveira,[‡] Karen F. Discola,[§] Simone V. Alves,[§] Francisco J. Medrano,[∥] Beatriz G. Guimarães,[⊥] and Luis E. S. Netto*[,§]

[‡]*Departamento de Biologia, Universidade Estadual Paulista, São Vicente, Brazil,* [§]*Departamento de Genética e Biologia Evolutiva, Instituto de Biociências, Universidade de São Paulo, São Paulo, Brazil,* [∥]*Departamento de Genética e Evolução, Instituto de Biologia, Universidade Estadual de Campinas, Campinas, Brazil, and* [⊥]*Synchrotron Soleil, L'Orme de Merisiers, Saint Aubin-BP48, Gif-sur-Yvette Cedex, France*

Received November 13, 2009; Revised Manuscript Received March 16, 2010

ABSTRACT: The enzymatic activity of thioredoxin reductase enzymes is endowed by at least two redox centers: a flavin and a dithiol/disulfide CXXC motif. The interaction between thioredoxin reductase and thioredoxin is generally species-specific, but the molecular aspects related to this phenomenon remain elusive. Here, we investigated the yeast cytosolic thioredoxin system, which is composed of NADPH, thioredoxin reductase (ScTrxR1), and thioredoxin 1 (ScTrx1) or thioredoxin 2 (ScTrx2). We showed that ScTrxR1 was able to efficiently reduce yeast thioredoxins (mitochondrial and cytosolic) but failed to reduce the human and *Escherichia coli* thioredoxin counterparts. To gain insights into this specificity, the crystallographic structure of oxidized ScTrxR1 was solved at 2.4 Å resolution. The protein topology of the redox centers indicated the necessity of a large structural rearrangement for FAD and thioredoxin reduction using NADPH. Therefore, we modeled a large structural rotation between the two ScTrxR1 domains (based on the previously described crystal structure, PDB code 1F6M). Employing diverse approaches including enzymatic assays, site-directed mutagenesis, amino acid sequence alignment, and structure comparisons, insights were obtained about the features involved in the species-specificity phenomenon, such as complementary electronic parameters between the surfaces of ScTrxR1 and yeast thioredoxin enzymes and loops and residues (such as Ser^{72} in ScTrx2). Finally, structural comparisons and amino acid alignments led us to propose a new classification that includes a larger number of enzymes with thioredoxin reductase activity, neglected in the low/high molecular weight classification.

Thioredoxin reductase is a member of the nucleotide pyridine disulfide oxidoreductase family, which includes glutathione reductase, alkyl hydroperoxide reductase F (AhpF)[1], and lipoamide dehydrogenase (*1*). Constituents of this family are homodimeric flavoproteins that also contain one or two dithiol−disulfide motifs, either CXXXXC or CXXC, or both (*1*−*5*). Thioredoxin reductase catalyzes the disulfide reduction of oxidized thioredoxin using NADPH via the FAD molecule and the redox-active cysteine residues (*6*). Thioredoxins are low molecular mass proteins (about 12 kDa) that are involved in central cellular processes such as the synthesis of deoxyribonucleotides, sulfur metabolism, regulation of gene expression, and oxidative stress defenses (*7*).

Thioredoxin reductase enzymes are widely distributed among all of the kingdoms and are commonly divided in two classes: the high molecular weight (HMW TrxRs) and low molecular weight (LMW TrxRs) thioredoxin reductase enzymes (*8*). HMW TrxRs are present in mammals, birds, insects, *Caenorabitis elegans*, and *Plasmodium falciparum* as dimers with a monomer molecular mass of approximately 55 kDa. Several HMW TrxRs have an additional redox center containing selenocysteine at the C-terminus (*9*, *10*).

LMW TrxRs are present in Archaea, bacteria, plants, and lower eukaryotes (such as yeasts) as dimers with a monomer molecular mass of approximately 33 kDa. In contrast with HMW TrxRs, the available three-dimensional structures of LMW TrxRs show the NADPH and FAD binding sites positioned on opposite faces of the molecule (*6*, *11*, *12*), making the transfer of electrons in this conformation (named FO for flavin oxidized) very unlikely. Furthermore, the dithiol−disulfide redox centers in these structures are buried deep in the polypeptide chain, creating a steric barrier for thioredoxin reduction. It was later shown that thioredoxin reductase from *Escherichia coli* can also adopt an alternative conformation designated FR (flavin reduced), allowing flavin reduction by NADPH (*13*). Transition between the FR and FO conformations is possible because the NADPH domain exhibits a 67° torsion relative to the FAD domain (*13*). In the FR conformation, FAD reduction by NADPH and reduction of the substrate (thioredoxin) by the thioredoxin reductase dithiol/disulfide redox are both feasible.

Saccharomyces cerevisiae has two thioredoxin reductase enzymes, which both belong to the LMW TrxRs class and are located in different compartments, the cytosol (ScTrxR1) and the

[†]Supported by FAPESP (Grant 07/58147-6; Grant 07/50930-3, Young Researchers in Emerging Centers) and CNPq (Grant 573530/08-4, Redox Processes in Biomedicine) and by the Brazilian Synchrotron Light Laboratory (Grant D03B-CPR-2197).

*To whom correspondence should be addressed. Tel: +55 11 3589 7589. Fax: +55 3091 7553. E-mail: nettoles@ib.usp.br.

[1]Abbreviations: AhpF, alkyl hydroperoxide reductase subunit F; EcTrx, *Escherichia coli* thioredoxin A; HMW TrxRs, high molecular weight thioredoxin reductases; HsTrx, *Homo sapiens* thioredoxin 1; LMW TrxRs, low molecular weight thioredoxin reductases; rmsd, root mean square deviation; ScTrx1, *Saccharomyces cerevisiae* thioredoxin cytosolic 1; ScTrx2, *S. cerevisiae* thioredoxin cytosolic 2; ScTrx3, *S. cerevisiae* thioredoxin mitochondrial 3; ScTrxR1, *S. cerevisiae* thioredoxin reductase cytosolic 1; ScTrxR2, *S. cerevisiae* thioredoxin reductase mitochondrial 2; TGR, thioredoxin glutaredoxin reductase; PDB, Protein Data Bank.

Published on Web 03/17/2010

mitochondria (ScTrxR2). Deletion of the ScTrxR1 gene, but not of the ScTrxR2 gene, rendered the cells unviable (*14*). ScTrxR1 is involved in the reduction of the two cytosolic thioredoxin isoforms (ScTrx1 and ScTrx2), which possess a high degree of amino sequence conservation between themselves (78% of identity and 89% of similarity).

In this work, we showed that ScTrxR1 was able to efficiently reduce ScTrx1, ScTrx2, and yeast mitochondrial thioredoxin (ScTrx3) but failed to reduce the *E. coli* thioredoxin A (EcTrx) and human thioredoxin 1 (HsTrx). To gain insights into this remarkable TrxR−Trx species specificity, we determined the crystallographic structure of a low molecular weight thioredoxin reductase from a fungus, *S. cerevisiae* (ScTrxR1). The structure revealed that the molecule is in the FO conformation. Additionally, the structure in the FR state was modeled based on the crystallographic structure of *E. coli* thioredoxin reductase complexed with thioredoxin (*13*) (PDB code 1F6M). Structural comparisons provided insights about substrate specificity. Some of the hypotheses raised were confirmed by enzymatic assays with ScTrx1 and ScTrx2 mutants, among them the role of the Ser^{72} (ScTrx2)/Ala^{71} (ScTrx1) residue in the specificity phenomenon. Finally, structural analyses together with sequence alignments provided arguments for the proposal of a new classification system for enzymes with thioredoxin reductase activity. Interestingly, ScTrxR1 residues involved in NADPH and FAD binding are highly conserved, whereas those residues involved in thioredoxin binding are highly variable.

EXPERIMENTAL PROCEDURES

Expression, Purification, and Crystallization. ScTrxR1 was expressed, purified, and crystallized as described before by Oliveira et al. (*39*).

Enzymatic Activity. ScTrxR1 activity toward various thioredoxin substrates was followed spectrophotometrically (ϵ_{412nm} = 13600 M^{-1} cm^{-1}) by the DTNB reduction assay (*10*). ScTrxR1 concentrations were fixed in all experiments at 0.03 μM. Thioredoxin concentrations were ranged from 0.1 to 8.0 μM. Reactions were initiated by the addition of 0.2 mM NADPH. Other reagents used in the assay included 0.1 mg/mL BSA, 0.25 mM DTNB, and 1 mM EDTA. The apparent kinetic constants were determined by nonlinear regression of Michaelis−Menten plots using the GraphPad Prism software. Measured activities in all assays were corrected by subtracting the velocities of the control reactions without thioredoxin, and three independent experiments were performed at each thioredoxin concentration.

Structure Solution and Refinement. The *S. cerevisiae* TrxR1 structure was solved by molecular replacement by means of the program AmoRe (*40*) using the atomic coordinates of *Arabidopsis thaliana* TrxR1 (PDB code 1VDC) as the search model. Structure refinement was performed using the program REFMAC 5.0 (*41*), and 5% of the data was set aside for cross-validation. Visual inspection of the electron density maps and model rebuilding were carried out with the program O (*42*). During the final cycles, water molecules were added both manually and using the program ARP/warp (*43*). The heterocompounds citrate and FAD were added to the model on the basis of the shape and difference density peaks in the $2F_o - F_c$ and $F_o - F_c$ density maps. The last three cycles of refinement were carried out using TLS (*44*). The coordinates have been deposited in the Protein Data Bank, accession number 3ITJ.

Analyses of the Primary, Tertiary, and Quaternary Structures. The multiple sequence alignment (MSA) was performed using ClustalX (*45*). Colors indicate the degree of similarity, which reflect physicochemical properties conserved for residues in each column based on the AMAS method of multiple sequence alignment analysis (*46*). The alignments are colored using Jalview (*47*). Dali (*48*) and VAST (*49*) were used for the comparison with protein tertiary structure coordinates deposited in protein structure database (http://www.rcsb.org). Tertiary and quaternary structure superpositions were carried out using the coordinates that had demonstrated significant structural similarity with *S. cerevisiae* TrxR1; they were carried out with the LSQKAB program from the CCP4 suite (Collaborative Computational Project, Number 4, 1994) (*50*) and SSM of the Coot program (*51*). Amino acid conservation in the protein structures was mapped using Consurf (*52*). The molecular representations were generated using Pymol (http://www.pymol.org).[2]

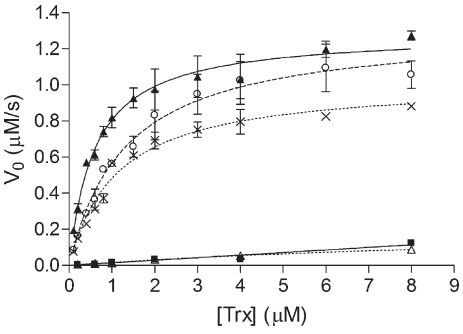

FIGURE 1: Species-specific reduction of thioredoxin enzymes by ScTrxR1. The reduction of ScTrx1 (- - -○), ScTrx2 (—▲), ScTrx3 (···×), HsTrx (···Δ), and EcTrx (—■) by ScTrxR1. Thioredoxin reductase concentration was fixed at 0.03 μM, and the concentrations of thioredoxins ranged from 0.1 to 8.0 μM. Reactions were initiated with the addition of 0.2 mM NADPH. Other reagents used in the assay included 0.1 mg/mL BSA and 0.25 mM DTNB. The apparent kinetic constants were determined by nonlinear regression of Michaelis−Menten plots using the GraphPad Prism software. No activity of ScTrxR1 was observed toward EcTrx and HsTrx, even when higher concentrations of these proteins were used (10 μM).

RESULTS AND DISCUSSION

ScTrxR1 Specifically Reduces Yeast Thioredoxin Enzymes. It has been assumed that thioredoxin reductase−thioredoxin interactions show species specificity, although no systematic investigation has been reported (*15*). The two cytosolic thioredoxin proteins from yeast (ScTrx1 and ScTrx2) share 78% amino acid identity and demonstrate 30% (ScTrx1) and 35% (ScTrx2) amino acid sequence identity relative to the EcTrx, 47% (ScTrx1) and 49% (ScTrx2) relative to HsTrx, and 46% (ScTrx1) and 43% (ScTrx2) relative to ScTrx3. In spite of these similarities, ScTrxR1 was able to specifically reduce both ScTrx1 and ScTrx2 with similar efficiency, whereas HsTrx and EcTrx displayed only slight activity (Figure 1). Furthermore, ScTrxR1 was also able to reduce mitochondrial ScTrx3 (Figure 1). ScTrxR1 displayed higher catalytic efficiency toward ScTrx2, mainly due to a lower K_M^{app} value (Table 1). Therefore, ScTrxR1 showed a very high species specificity toward the yeast thioredoxin enzymes among other thiol−disulfide oxidoreductases. Molecular aspects of this

[2]During the preparation of the manuscript, the crystal structure of ScTrxR1 was reported by Zhang et al. (*53*). The two structures are identical, but no detailed investigation of the substrate species specificity (including the enzymatic activities of ScTrxR1 toward various thioredoxin substrates, as well as site-directed mutagenesis studies) was performed in ref *53*.

specificity were investigated here through structural and biochemical analyses.

Overall Structure of ScTrxR1. To gain insights into the ScTrxR1−ScTrx1/ScTrx2 interactions, the crystal structure of ScTrxR1 has been refined at 2.4 Å resolution to an R_{factor} of 0.169 (R_{free} = 0.194). The asymmetric unit is composed of four monomers, named A, B, C, and D, which form a cross-shaped structure (Figure 2A).

The quality of electron density maps allowed the modeling of 317, 318, 314, and 307 residues of monomers A, B, C, and D, respectively (out of 318 residues). Most of the lack in electron density was found in monomers C and D and included their active sites. The final model includes 1257 amino acids, 50 of which were assigned as alanine (40 located in monomers C and D). The final model has good overall stereochemistry. All non-glycine and non-proline residues fall in the most favored or additionally allowed regions of the Ramachandran plot as defined by the program PROCHECK (*16*). Crystal data and final model statistics are reported in Table 2. The Cα rmsd among the four monomers in the asymmetric unit are in the range 0.37−1.69 Å (B/A = 0.37, B/C = 1.13, B/D = 1.64, A/C = 1.22, A/D = 1.61, and C/D = 1.69). Despite the slight differences, the monomers are structurally identical, and therefore we will use monomer B to describe the structure of ScTrxR1.

Table 1: Apparent Kinetic Parameters for Reduction of Thioredoxins by ScTrxR1[a]

	K_M^{app} (μM)	k_{cat}^{app} (s^{-1})	k_{cat}/K_M
Trx1−TrxR1	1.3 ± 0.2	43.7 ± 2.5	(3.4 ± 1.2) × 10^7
Trx2−TrxR1	0.6 ± 0.1	42.9 ± 1.5	(7.3 ± 1.5) × 10^7
Trx3−TrxR1	1.1 ± 0.1	34.0 ± 1.1	(3.1 ± 1.1) × 10^7
Trx human−TrxR1	nd	nd	nd
Trx *E. coli*−TrxR1	nd	nd	nd

[a]Parameters determined by nonlinear regression from data presented in Figure 1 and fitted by the Michaelis−Menten equation (GraphPad). nd, not determined.

The ScTrxR1 monomer is composed of two β-α-β-α-β domains that form the binding sites of NADPH and FAD (Figure 2B) similar to the Archaea, bacteria, and plant counterparts (*6*, *8*, *12*, *17*). The FAD binding domain is composed of residues 1−121 (β strands 1−8 and α helices 1−3) and 253 −318 (β strand 19 and α helices 9−11). A FAD molecule is bound to the ScTrxR1 structure and is stabilized by interactions with the residues Pro[13], Glu[33], Gln[45], Asn[54], Gln[136], Asp[288], and Gln[296]. The FAD interactions are very similar to those found in LMW TrxRs of other organisms (*6*, *8*, *12*, *17*).

The NADPH binding domain is a continuous sequence (from residue 123 to residue 250) and is composed of β strands 10−17 and α helices 5−8. Curiously, a strong electron density, which does not correspond to water molecules, was observed at the NADPH binding site. Two citrate molecules (Figure 2C) that probably come from the crystallization mother liquor solution fitted well into these electronic densities (Supporting Information, Figure S1). These citrate molecules are stabilized by several polar interactions with the side or main chain amines of residues Lys[124], Ser[165], Arg[185], Lys[186], Arg[190], and His[250].

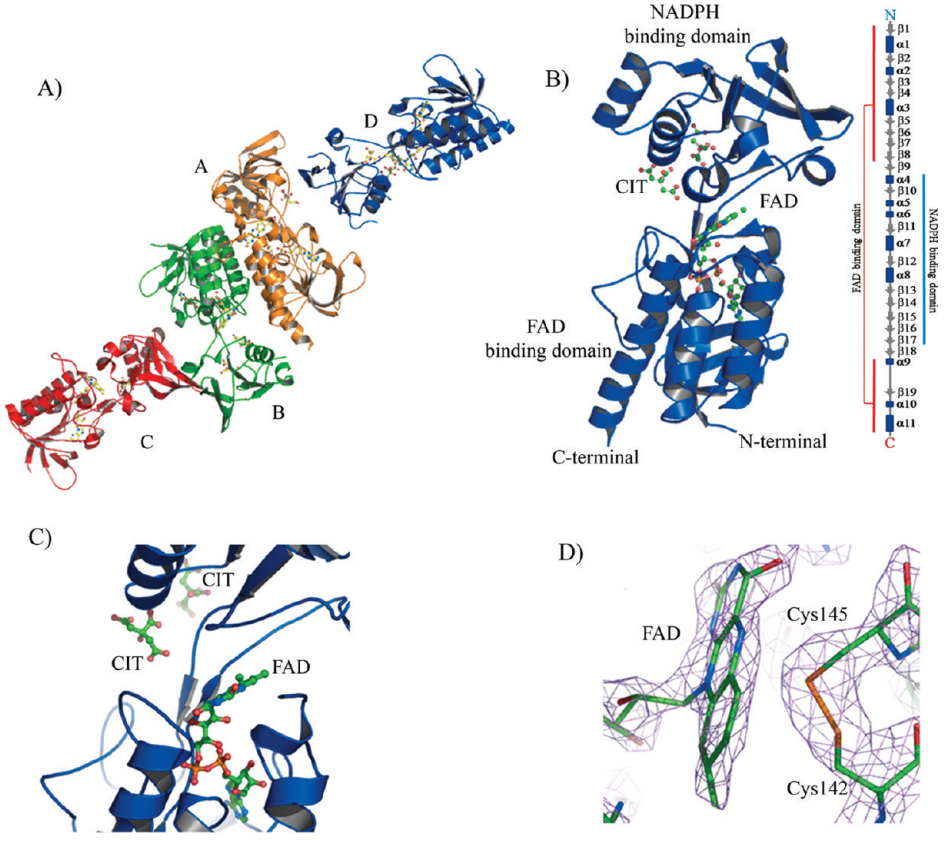

FIGURE 2: ScTrxR1 structure. (A) The asymmetric unit of yeast TrxR1 is composed of four monomers (named A, B, C, and D) forming a cross-shaped structure. The monomers are represented by different colors. (B) The ScTrxR1 monomer structure, colored in blue, shows both NADPH and FAD binding domains composed of a β-α-β-α-β fold. A linear representation of the secondary structure assignment is shown at the right side, and the N- and C-termini are indicated in the model. (C) Close-up view of the NADPH binding site occupied by two citrate molecules. (D) Final $2F_o - F_c$ map contoured at 1.5σ showing the FAD electron density and the Cys142-Cys145 disulfide. The FAD molecule and catalytic cysteines are in ball and stick format.

Table 2: Crystallographic Data and Refinement Statistics[a]

space group	*C*2
unit cell parameters	
a, *b*, *c* (Å)	127.97, 135.41, 75.81
β (deg)	89.95
resolution limits (outer shell) (Å)	46.6−2.4 (2.46−2.40)
no. of total reflections	297954
no. of unique reflections	48181
completeness (%)	99.6 (99.7)
multiplicity	6.1 (6.0)
R_{sym}[b] (%)	9.9 (32.5)
$\langle I/\sigma(I)\rangle$	5.8 (2.2)
reflections	
working	46488
test	2459
non-hydrogen atoms	
protein	9270
heteroatoms (FAD and citrate)	302
waters	277
R_{factor}/R_{free} (%)	16.91/19.40
rmsd	
bonds (Å)	0.024
angles (deg)	2.25
average *B* factor	
main chain	19.62
side chains and waters	22.77
Ramachandran analysis (%)	
most favored regions	85.6
additionally allowed regions	14.4
PDB code	3ITJ

[a]Values in parentheses refer to the highest resolution shell. [b]$R_{sym} = \sum_{hkl}\sum_i |I_{hkl,i} - \langle I\rangle_{hkl}|/\sum|\langle I\rangle_{hkl}|$.

The two domains are linked by a short β sheet composed of strands 9 and 18. Interestingly, the two domains themselves share substantial structural similarities (rmsd of 2.59 Å for 83 superposed Cα atoms as calculated by SSM (*18*)). Structural similarities between the two domains are in agreement with the suggestion that these domains arose from a gene duplication event (*19*).

The redox-active cysteine residues (Cys[142]-Ala-Val-Cys[145]) are found in a loop located between β10 and α5 of the NADPH domain and form a disulfide bond (Sγ−Sγ distance = 2.1 Å), which is close to the flavin ring (Figure 2D). However, the catalytic cysteines are buried in the NADPH domain, creating a steric barrier for thioredoxin interaction. Additionally, the NADPH binding site (occupied in the ScTrxR1 crystal structure by two citrate molecules) is too far away to transfer reducing equivalents to the flavin ring. This kind of organization is similar to the FO conformation previously described for thioredoxin reductases from Archaea, bacteria, and plant organisms (*6*, *8*, *12*, *17*). Due to its similarity to other LMW TrxRs, the probable biological unit of ScTrxR1 is a homodimer (*1*), and it is represented by monomers A and B (Figure 2A) with an interface area between the monomers of ∼2040 Å^2 as calculated by the PISA program (*20*). From this analysis, it is clear that the dimer is stabilized by a large number of hydrophobic and polar interactions (Supporting Information, Figure S2).

Molecular Modeling of ScTrxR1 in the FR Conformation. In order to study the electron transfer process in ScTrxR1, the atomic coordinates of the *E. coli* thioredoxin reductase−thioredoxin complex (PDB code 1F6M) were used to model the corresponding FR conformation for ScTrxR1. Initially, the FAD and NADPH binding domains were separated, and the β7−β16 sheet linker was excluded. After superposition of the ScTrxR1 and *E. coli* NADPH domains, the two domains were then rejoined, and with a few adjustments, it was possible to model the FAD domain in an equivalent position to that seen in the *E. coli* complex, following a procedure similar to that described by Akif et al. (*8*). As previously observed for *E. coli* thioredoxin reductase (*13*), no steric barriers to the proposed rotation were encountered that could not be surmounted by the adjustment of side chains. Superposition of the FR structures resulted in an rmsd of 1.13 Å for the 120 aligned α-carbon atoms (out of 125). As expected, the ∼67° rotation brings the NADPH binding site to the FAD molecule and exposes the active cysteines to the thioredoxin reduction (Figure 3B,D). For the reduction of the ScTrxR1 disulfide by $FADH_2$, a counter-rotation should occur (Figure 3C).

Structural Analyses of ScTrxR1−Thioredoxin Interactions. To investigate the features involved in the remarkable ScTrxR1−ScTrx1 or ScTrxR1−ScTrx2 species-specific reduction (Figure 1), we analyzed the surface of ScTrxR1. The FR model shows a distribution of charges at the thioredoxin-interacting face, with a positive charge at an extremity (named region A) and two negative ones (named B and C) in other positions of ScTrxR1 surface (Figure 4). These three regions at the ScTrxR1 surface can potentially interact with complementary regions of the thioredoxin enzymes (regions A′, B′, and C′) when taking into account the structure of the thioredoxin reductase−thioredoxin complex from *E. coli* (PDB code 1F6M). The ScTrxR1 region A displayed a positive net charge, which is in part produced by the side chain of amino acids Arg[153], Lys[175], and Lys[137] and the main chain of Ile[139]. The Trx counterpart region (A′) differs significantly between yeast Trx (ScTrx1, ScTrx2, and ScTrx3) and EcTrx, while HsTrx possesses intermediate properties (Figure 4).

Region B in the ScTrxR1 structure is negatively charged, whereas B′ is positively charged in all of the analyzed thioredoxin enzymes. Regions B and B′ possess the catalytic cysteines of ScTrxR1 and the thioredoxin enzymes, respectively. Finally, region C is also negatively charged in ScTrxR1, and C′ has a positive electrostatic potential that is similar in yeast and HsTrx but again differs in EcTrx. The charge distribution can partially explain the lower activity of ScTrxR1 toward EcTrx. However, this analysis provided no evidence for the absence of ScTrxR1 activity toward HsTrx. Therefore, other features were investigated.

In addition to the electronic surface properties, three ScTrxR1 loops (named here X, Y, and Z and shown as blue structures in Figure 4B) appear to be relevant in recognition of the yeast thioredoxin enzyme surface. Loop Z is positioned at one extremity of ScTrxR1 and is composed of segment 216-AKGDGKLLN-224. Compared to the yeast thioredoxin enzymes, loop Z was not well accommodated by the HsTrx and EcTrx surfaces, since a larger space can be observed between the two proteins (Figure 4B). Loop X is shorter and contains amino acids 83−88 (ITETVS); it can interact with basic residues such as those contained in the positively charged region C′ of thioredoxins. This segment is not conserved in EcTrxR (80-IFDHIN-85) and HsTrxR (127-YENAYG-132). As seen with loop Z, loop X also did not appear to fit well in the HsTrx and EcTrx surfaces (Figure 4B).

Loop Y is directly related to substrate reduction since it contains the catalytic cysteine residues and Asp[146], which is apparently involved in substrate recognition and/or acid−base catalysis (see description below of Figure 5). Furthermore, loop Y is positioned in between loops 2 and 3 of the Trx proteins (shown as green and red structures in Figure 4B), and its amino acid sequence is very divergent from other LMW TrxRs (see results

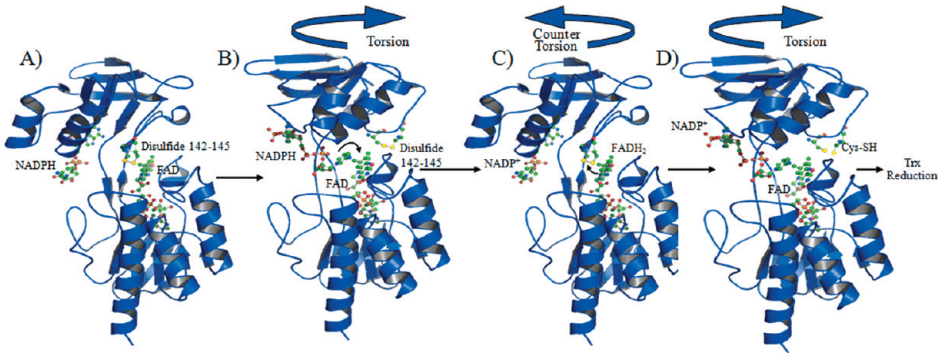

FIGURE 3: Molecular modeling of the NADPH domain rotation. (A) ScTrxR1 in the FO state shows the catalytic cysteines oxidized to a disulfide bond and buried in the protein structure. NADPH and FAD are far away from each other. (B) A large rotation of about 67° places the NADPH molecule close to the FAD molecule (adopting the FR state), allowing the hydride transfer to the flavin (C) counter-rotation (back to FO state) approximating $FADH_2$ to the disulfide bond of the ScTrxR, allowing its reduction and then (D) another rotation (to FR state), bringing the buried cysteines to the solvent surface, which allows thioredoxin reduction. The conformation of FR has been modeled based on the corresponding conformation of the *E. coli* complex TrxR−Trx and $AADP^+$ (an NADPH analogue) (PBD code 1F6M). Sulfur atoms in the catalytic cysteines of TrxR1 are represented in yellow.

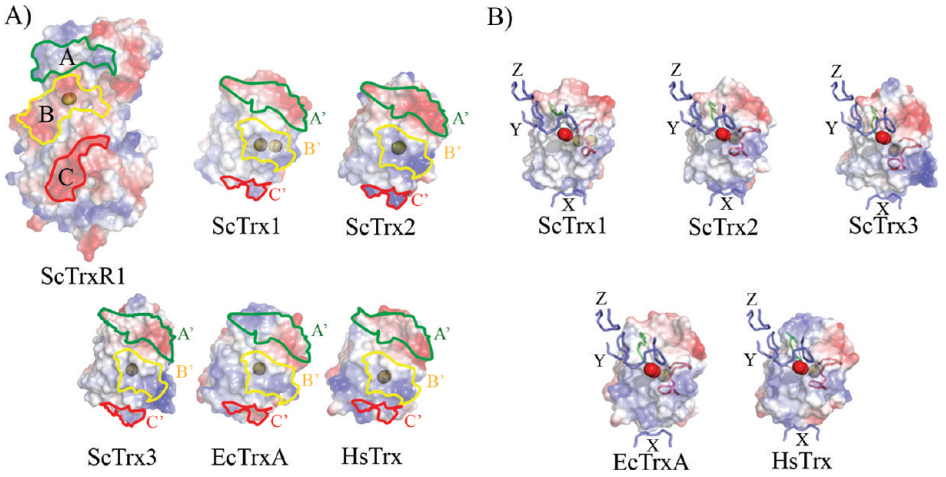

FIGURE 4: Complementary electrostatic surfaces of the ScTrxR1 and Trx loops. (A) Electrostatic surfaces of ScTrxR1, ScTrx1 (PDB code 2I9H), ScTrx2 (PDB code 2FA4), ScTrx3 (PDB code 2OE3), HsTrx1 (PDB code 1ERU), and EcTrx (PDB code 1XOA) are colored by charge from red (negative) to blue (positive). Three complementary contact areas between thioredoxin reductase and thioredoxin from yeast can be identified and are labeled A−A′, B−B′, and C−C′ (highlighted in green, yellow, and red, respectively). These regions were chosen by taking into account the structure of the thioredoxin reductase−thioredoxin complex from *E. coli* (PDB code 1F6M). The catalytic cysteine residues are represented by spheres. The structures of ScTrx1, ScTrx2, ScTrx3, HsTrx1, and EcTrx are in the oxidized state, while the cysteine residues of ScTrxR1 are in the reduced state. (B) Accommodation of the ScTrxR1 loops into the surface of ScTrx1, ScTrx2, ScTrx3, HsTrx1, and EcTrx proteins. Thioredoxin loops 2 and 3 are colored red and green, respectively, according to nomenclature described in Figure 5. Positive and negative charges are represented by blue and red colors, respectively. The ScTrxR1 loops are colored in blue and labeled as X, Y, and Z. Catalytic cysteine residues are represented by red spheres in ScTrxR1 (loop X) and orange spheres in the Trx proteins (loop 2).

below and Supporting Information, Figure S4). Therefore, loops X, Y, and Z appear to be relevant features for ScTrxR1's recognition of its thioredoxin partner.

In addition to electronic surfaces and ScTrxR1 loops, thioredoxin loops appear to be important for protein−protein interactions. Recent structural analyses have revealed that yeast cytosolic thioredoxin enzymes contain three highly flexible loops, loop 1 (17-SGDK-20), loop 2 (28-ATWCGPCK-35), and loop 3 (68-AEVSSMP-74), which could also be implicated in substrate interactions (*21*, *22*). The amino acid sequence of loop 2 (that contains the catalytic cysteine residues) is highly conserved in all thioredoxin enzymes, which contrasts with the sequence variability of loops 1 and 3 (Figure 5A). Another indication that loop 3 is a relevant feature for substrate specificity in the thioredoxin−thioredoxin reductase interactions comes from the molecular dynamics simulation and protein−protein docking studies along with site-directed mutagenesis, showing that Arg^{73} from EcTrx is important for its productive binding to thioredoxin reductase from *E. coli* (*23*). Interestingly, Arg^{73} is not conserved in yeast thioredoxin (Ser in ScTrx1 and ScTrx2, Thr in ScTrx3) and is present in loop 3 of EcTrx (Figure 5).

Additional analyses using the FR model indicated that residues present in thioredoxin loops 2 and 3 may in fact provide interacting elements with ScTrxR1 (Figure 5B). Two charged residues of ScTrxR1, Lys^{137} and Asp^{146}, appear to interact with Glu^{69} and Ser^{72} (from loop 3), respectively, of ScTrx 2. The residues in this loop are relatively conserved between the two cytosolic yeast thioredoxin enzymes, and similar interactions can occur with both (Figure 5A). In contrast, residues equivalent to Ser^{72} of ScTrx2 vary among the thioredoxin enzymes. Since loop 1 is very far from the interacting regions and loop 2 is highly conserved among the five proteins, loop 3 is probably one of the features involved in the species specificity of the reductions carried out by ScTrxR1 (Figure 5).

To test this hypothesis, ScTrxR1K137A and ScTrxR1D146A were generated by site-directed mutagenesis, and their ability to

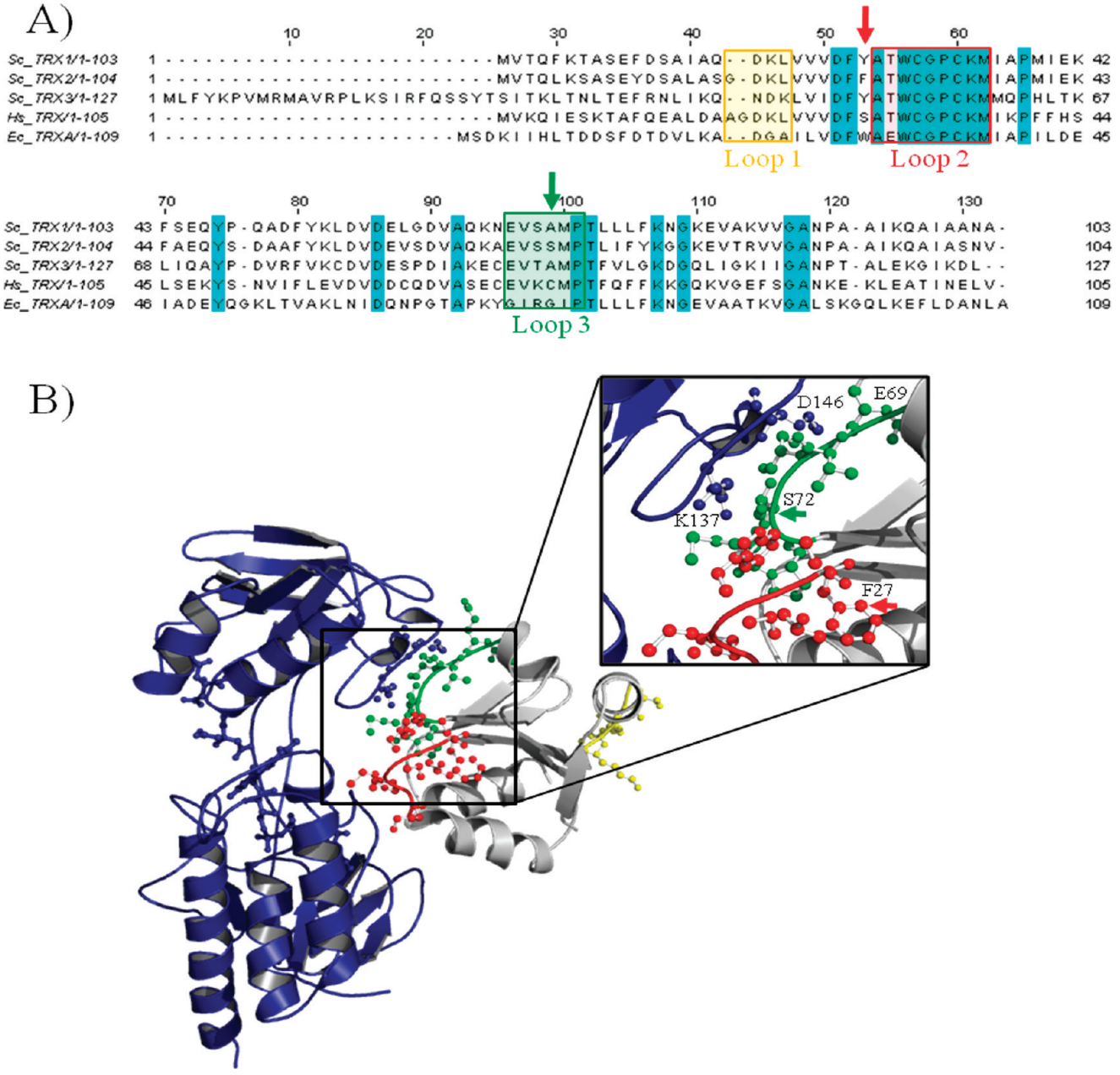

FIGURE 5: Thioredoxin loops involved in TrxR interaction. (A) Alignment of the amino acid sequences of ScTrx1, ScTrx2, ScTrx3, HsTrx, and EcTrx. Identical residues are highlighted in cyan, and the colored boxes denote the three flexible interacting loops (yellow, loop 1; red, loop 2; green, loop 3). Alignments were performed using ClustalX software (*39*). (B) The ScTrxR1 FR model (blue) and the crystal structure of ScTrx2 (gray) were individually superposed over the corresponding *E. coli* complex (PDB code 1F6M). ScTrx2 Glu^{69} and Ser^{72} from loop 3 can form polar interactions with Lys^{137} and Asp^{146} from ScTrxR1. The Trx loop residues are represented as balls and sticks in yellow (loop 1), red (loop 2), and green (loop 3). The green and red arrows show the position of ScTrx2F27 and ScTrx2S72 (A and B), and residues are represented as balls and sticks (B).

reduce ScTrx2 was evaluated. The replacement of Asp^{146} by alanine resulted in the abolishment of thioredoxin reductase activity (Figure 6A), which could indicate that this residue is relevant for substrate recognition by ScTrxR1 through its interaction with Ser^{72} of ScTrx2 (Figure 5B). However, the interpretation of this result is complex, since Asp^{140} from *E. coli* thioredoxin reductase (equivalent to Asp^{146} in ScTrxR1) functions as an acid−base catalyst (*24*). Nevertheless, this is the first description of the essential role of the Asp residue in catalysis for a eukaryotic LMW TrxR.

On the other hand, the Lys^{137} substitution to alanine did not alter the ScTrxR1 activity toward ScTrx2 (Figure 6A), indicating that this residue in not relevant for substrate interaction. In any case, we cannot exclude the possibility that ScTrxR1 Lys^{137} is involved in the thioredoxin reduction, since Kirkensgaard et al. (*25*) observed that EcTrxR Gly^{129}, Arg^{130}, and Ala^{237} provide all five of the hydrogen bonds formed upon Trx binding (EcTrxR Arg^{130} is equivalent to ScTrxR1 Lys^{137}). Interestingly, the residues immediately before the corresponding ScTrxR1 Lys^{136} vary considerably among the LMW TrxRs ($W^{135}Q^{136}$ in yeast, $K^{129}G^{130}$ in *E. coli*, $W^{140}N^{141}$ in *A. thaliana*) and could contribute to the specificity described here.

While further analyzing the reduction of thioredoxin proteins, we observed that ScTrxR1 displayed a lower K_M^{app} for the reduction of ScTrx2 than for the reduction of ScTrx1 (Figure 1), corresponding to an increased catalytic efficiency for the former substrate (Table 1). A small divergence in the amino acid sequences in both loop 2 (a single substitution of ScTrx1 Tyr^{26}

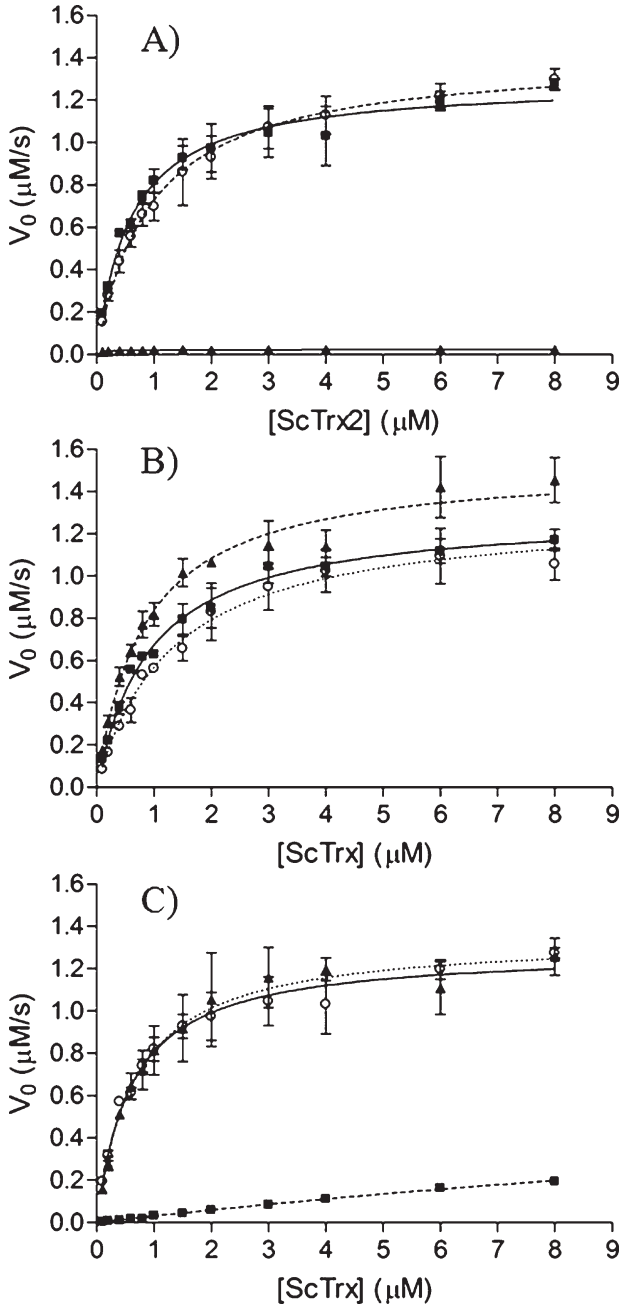

FIGURE 6: Enzymatic properties of the site-specific mutants of ScTrxR1 (A), ScTrx1 (B), and ScTrx2 (C). All reactions were followed spectrophotometrically by the DTNB reduction assay (A_{412nm}) and were initiated with the addition of 0.2 mM NADPH. The apparent kinetic constants were determined by nonlinear regression of Michaelis−Menten plots using the GraphPad Prism software. (A) Reduction of ScTrx2 by ScTrxR1 (—■), ScTrxR1K137A (- - -○), and ScTrxR1 D146A (—▲). (B) Reduction of ScTrx1 (·····○), ScTrx1Y27F (- - -▲), and ScTrx1A71S (—■) by ScTrxR1. (C) Reduction of ScTrx2 (·····○), ScTrx2F27Y (—▲), and ScTrx2S72A (—■) by ScTrxR1. Final concentrations used in the assay: ScTrxR1, 0.03 μM; ScTrxs, from 0.1 to 8.0 μM; BSA, 0.1 mg/mL; DTNB, 0.25 mM.

by a Phe[27] in ScTrx2) and loop 3 (two substitutions: Asn[67] and Ala[71] in ScTrx1 and Ala[68] and Ser[72] in ScTrx2) might contribute to the differences observed in the catalytic process (Figure 1). To test this hypothesis, site-specific mutants were generated, replacing the residues present in loops 2 and 3 of ScTrx1 and ScTrx2.

The replacement of Ser[72] with Ala impaired the ability of ScTrxR1 to reduce ScTrx2, whereas the substitution of Ala[71] with Ser in ScTrx1 increased ScTrxR1 activity (Figure 6B,C; Table 3). These data strongly implicated Ser[72] in the higher reduction rate of ScTrx2 in the process catalyzed by ScTrxR1, corroborating our structural analyses.

Table 3: Effect of Mutations on Apparent Kinetic Parameters for the Reduction of Thioredoxin by ScTrxR1[a]

	K_M^{app} (μM)	k_{cat}^{app} (s^{-1})	k_{cat}/K_M
Trx2−TrxR1	0.6 ± 0.1	42.9 ± 1.5	(7.3 ± 1.5) × 10^7
Trx2−TrxR1K137A	0.9 ± 0.1	47.1 ± 2.0	(5.2 ± 2.0) × 10^7
Trx2−TrxR1D146A	nd	nd	nd
Trx2F27Y−TrxR1	0.7 ± 0.1	45 0.0 ± 2.3	(6.7 ± 2.3) × 10^7
Trx2S72A−TrxR1	28 ± 5[b]	30.1 ± 4.3[b]	(1.1 ± 0.1) × 10^6 [b]
Trx1−TrxR1	1.3 ± 0.2	43.7 ± 2.5	(3.4 ± 1.2) × 10^7
Trx1Y27F−TrxR1	0.9 ± 0.1	52.7 ± 2.1	(5.8 ± 2.1) × 10^7
Trx1A71S−TrxR1	0.9 ± 0.1	43.4 ± 1.3	(4.8 ± 1.3) × 10^7

[a]Parameters determined by nonlinear regression from data presented in Figures 1 and 6 and fitted by the Michaelis−Menten equation (GraphPad). nd, not determined. [b]We could not achieve saturating concentrations of Trx2-S72A; thus these data are only an estimation.

The role of Phe[27](ScTrx2)/Tyr[26](ScTrx1) in this process is not as clear. Although the replacement of Tyr[26] with Phe in ScTrx1 resulted in augmentation of the ScTrx1 reduction rate (Figure 6B, Table 3), the replacement of Phe[27] with Tyr in ScTrx2 provoked no effect (Figure 6C, Table 3). Nevertheless, when taken together, the results presented here (Table 3, Figures 1, 5, and 6B,C) indicate that ScTrxR1's reduction of ScTrx2 is slightly more efficient that its reduction of ScTrx1. Differences in the ability of ScTrx1 and ScTrx2 to interact with other proteins (peroxiredoxins and phosphoadenosine 5-phosphosulfate) have also been described recently (*26*).

Structural Comparisons and a New Classification Proposal. Next, crystal structures of LMW TrxRs in the FO conformation were compared by secondary structure matching (SSM), followed by Cα alignment using the SSM−Coot routine. LMW TrxR crystal structures share a high degree of structural similarity except for insertions or deletions in some loops. Superposition of the ScTrxR1 structure with its LMW TrxR counterparts from *A. thaliana* (1VDC, 63% identity), *E. coli* (1TDE, 50% identity), and *Mycobacterium tuberculosis* (2A87, 47% identity) resulted in overall rmsd of 0.876 Å (310 Cα aligned), 1.246 Å (301 Cα aligned), and 1.125 Å (302 Cα), respectively (Supporting Information, Figure S3A).

Although AhpFs (about 57 kDa) are larger than the LMW TrxRs (about 33 kDa), an AhpF domain ranging approximately from residue ~200 to residue 520 (*3*, *27*, *28*), which corresponds to the NADPH and FAD binding domains, shares high degree of structural similarity with ScTrxR1 (Supporting Information, Figure S3B). AhpF proteins possess an additional N-terminal domain composed of two contiguous thioredoxin folds with an eight-strand β sheet and five α helices (Supporting Information, Figure S3B). All of the LMW TrxR structures are in the FO conformation (Supporting Information, Figure S3A,B), and similar to the AhpF proteins, they show FAD molecules and catalytic cysteines in equivalent positions. Therefore, the domains shared by AhpF and LMW TrxR were designated herein as "the catalytic core" (NADPH and FAD binding domains) of thioredoxin reductases. Structural superposition of AhpF and ScTrxR1 gives an overall rmsd of 1.685 Å (281 Cα aligned) for *E. coli* AhpF, whose crystallographic structure comprises only the catalytic core, and 1.772 Å for the *Salmonella typhimurium* AhpF full protein structure (299 Cα aligned).

Additional domains attached to the catalytic core are not an exclusive feature of AhpF proteins. Thioredoxin reductase from

Mycobacterium lepreae is unusual and possesses a thioredoxin molecule attached to its C-terminal portion (*29*, *30*). Sequence alignment using the BlastP program (http://www.ncbi.nlm.nih.gov/blastp) revealed several proteins or hypothetical proteins that displayed this feature. Thioredoxin modules linked to the catalytic core are present in eubacteria, cyanobacteria, and plants, but, unfortunately, there are no structures for these proteins available to date. Additionally, the structural comparison of the biological units (dimer) strengthens the hypothesis that ScTrxR1 is strictly related to AhpF, since the interactions that maintain the biological units are conserved (Supporting Information, Figure S2C).

Interestingly, although the ScTrxR1 crystal structure, which is in the FO conformation, does not show overall structural similarity with the mammalian TrxRs (belonging to HMW TrxR group), the FR ScTrxR1 model revealed structural conservation between the LMW and HMW TrxRs (Supporting Information, Figure S3C). This same conservation was observed when the FR ScTrxR1 model was aligned with other nucleotide pyridine disulfide oxidoreductase structures such as glutathione reductase and lipoamide dehydrogenase proteins (Supporting Information, Figure S3D). In addition to the NADPH and FAD domains, HMW TrxR enzymes possess a third domain, called the interface or dimerization domain, which is composed of approximately 150 residues at the C-terminus and accounts for the difference in molecular weight between LMW and HMW TrxRs. The presence of the dimerization domain also results in major differences in the structural organization of the assembly of the two subunits (Supporting Information, Figure S3E), which reflect variations with regard to the electron transference between LMW TrxR and HMW TrxR enzymes, including an additional redox center (an active disulfide or selenyl sulfide) in the dimerization domain (*31*, *32*).

Another group of thioredoxin reductase enzymes possesses additional domains similar to glutaredoxin that are attached to the HMW TrxR architecture. These enzymes, such as TGR from *Schistosoma mansoni* and isoforms of mammalian TrxRs, are the products of alternative splicing (*33*, *34*). AhpF and TGR are examples of enzymes that possess thioredoxin reductase activity but that cannot be easily categorized as either LMW or HMW TrxRs.

Although the properties of the thioredoxin reductase enzymes are diverse, amino acid sequence alignments and structural analysis indicated a high degree of conservation of "the catalytic core" (Supporting Information, Figure S4). Therefore, a new classification system is proposed here and is based on the structural organization of different groups around the catalytical core (Figure 7). According to our proposal, instead of the classical division of thioredoxin reductase enzymes in the LMW TrxR and HMW TrxR groups, they should be separated into five categories, including AhpF and thioredoxin reductases with N- or C-terminal extensions not covered by the traditional classifications (Figure 7, Table 4). Therefore, this proposal includes more enzymes than the initial system of HMW TrxR and LMW TrxR groups.

Analyses of the ScTrxR1 FR model using the Consurf program indicated that the most conserved residues are positioned at the center of the enzyme and the poorly conserved regions are situated at the extremes of the molecule (Supporting Information, Figure S5). The most conserved residues are positioned mainly inside the molecule and are involved in interactions with the FAD (Supporting Information,Figure S5C) and NAD(P)H (Supporting Information,Figure S5C) molecules that are present in the thioredoxin reductase−thioredoxin interactions in

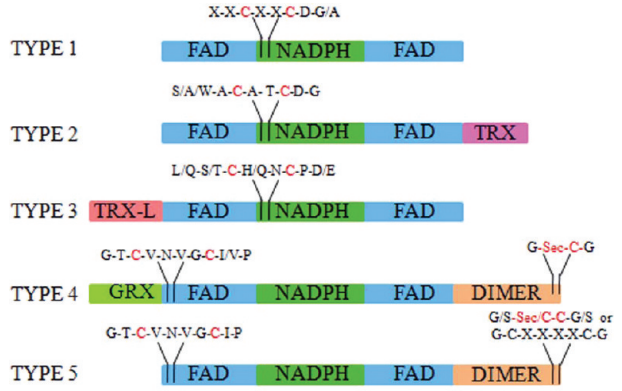

FIGURE 7: Classification of the thioredoxin reductase enzymes. The diagram shows the organization of the elements and domains in the five TrxR types. In types 1, 2 and 3, the catalytic cysteines belong to the NAD(P)H domain. In types 4 and 5, the cysteines are found in the FAD domain.

all organisms. This is consistent with the fact that TrxR interactions with these low molecular weight compounds should be very similar throughout the different taxonomic groups.

In contrast, although all thioredoxin reductases share considerable structural similarity, they do display different properties. Remarkably, the amino acid composition of the molecular surface of these enzymes exhibits a high degree of diversity (Supporting Information, Figure S5). In line with this rationale, the extremes of the thioredoxin reductase surfaces display increased variation, which possibly reflects the variation in the properties of thioredoxin from different organisms and is probably at least partially involved in the species specificity of this interaction (Figure 1).

Although some sporadic observations of species specificity in TrxR−Trx interactions have been made, no systematic investigations have been carried out. For instance, while the thioredoxin reductase from *E. coli* can reduce only *E. coli* Trx1 and *E. coli* Trx 2, but not ScTrx3 (*35*), thioredoxin reductase from mammals can reduce thioredoxin enzymes from other species (*35*, *36*). In this case, thioredoxin reduction is achieved in HMW TrxRs by the C-terminal extension containing the additional redox center with a second disulfide or a selenenyl sulfide (*32*). Therefore, the species specificity phenomenon appears to strictly be a feature of LMW TrxRs.

In addition to species specificity, organellar specificity also appears to be relevant; a mitochondrial thioredoxin from a plant is more efficiently reduced by mitochondrial thioredoxin from yeast (ScTrxR2) than by cytosolic thioredoxin reductase from the same plant (*37*). Recently, it was shown that nematode thioredoxin is reducible not only by thioredoxin reductase but also unexpectedly by the glutathione−glutathione reductase pathway (*38*), indicating that several aspects of these protein−protein interactions still need to be elucidated.

In summary, despite some observations of species-specific interactions, the molecular basis involved in the phenomenon is still elusive. Therefore, this work contributed to the better comprehension of the species specificity phenomenon. Initially, we clearly defined the specificity of ScTrxR1 for various thioredoxin enzymes (Figure 1). Insights into this phenomenon were then presented, which involved complementary electronic parameters between the surfaces of ScTrxR1 and the yeast thioredoxin enzymes (Figure 4A) and the identification of loops (Figures 4B and 5) and residues (such as Ser^{72} in ScTrx2) involved

Table 4: Features of the Thioredoxin Reductase Enzyme Types[a]

type	molecular mass (per subunit, kDa)	consensus of motif containing catalytic Cys	extra domains and catalytic motifs	representatives
1	35	X-X-C-X-X-C-D-G/A[b]	no	ScTrxR1, bacteria, plant
2	42	S/A/W-A-C-A/T-C-D-G[c]	Trx C-terminal	*M. leprae*, cyanobacteria, and some plants
3	57	L/Q-S/T-C-H/Q-N-C-P-D/E[d]	Trx N-terminal	bacterial AhpF
4	55	G-T-C-V-N-V-G-C-I/V-P[e]	SeCys C-terminal (dimerization domain/C-terminal catalytic motif: G-SeCys-C-G)	human TrxR1 isoform 3, TGR from *S. mansoni* and *E. granulosus*
5	65	G-T-C-V-N-V-G-C-I-P[f]	(a) Trx N-terminal; (b) SeCys C-terminal (dimerization domain/ C-terminal catalytic motif: G/S-Sec/ C-C-G/S or G-C-X-X-X-X-C-G in some protozoan)	human TrxR1 isoforms 1 and 2, vertebrates, insects, and protozoan

[a]Trx = thioredoxin; TGR = thioredoxin glutathione reductase. [b]Consensus obtained by the alignment of 200 amino acid sequences. [c]Consensus obtained by the alignment of 35 amino acid sequences. [d]Consensus obtained by the alignment of 60 amino acid sequences. [e]Consensus obtained by the alignment of 20 amino acid sequences. [f]Consensus obtained by the alignment of 15 amino acid sequences.

in protein−protein interactions (Figures 5 and 6 and Supporting Information, S5). These findings are relevant in the context of redox signaling where the partners for different oxidoreductases vary and also in drug development since the thioredoxin reductases from pathogens possess very distinct properties from the mammalian counterparts.

SUPPORTING INFORMATION AVAILABLE

Five figures as described in the text. This material is available free of charge via the Internet at http://pubs.acs.org.

REFERENCES

1. Williams, C. H., Jr., Arscott, L. D., Muller, S., Lennon, B. W., Ludwig, M. L., Wang, P. F., Veine, D. M., Becker, K., and Schirmer, R. H. (2000) Thioredoxin reductase: Two modes of catalysis have evolved. *Eur. J. Biochem. 267*, 6110–6117.
2. Ermler, U., and Schulz, G. E. (1991) The three-dimensional structure of glutathione reductase from *Escherichia coli* at 3.0 Å resolution. *Proteins 9*, 174–179.
3. Ledwidge, R., Patel, B., Dong, A., Fiedler, D., Falkowski, M., Zelikova, J., Summers, A. O., Pai, E. F., and Miller, S. M. (2005) NmerA, the metal binding domain of mercuric ion reductase, removes Hg(2+) from proteins, delivers it to the catalytic core, and protects cells under glutathione-depleted conditions. *Biochemistry 44*, 11402–11416.
4. Rajashankar, R. K., Bryk, R., Kniewel, R., Buglino, J. A., Nathan, C. F., and Lima, C. D. (2005) Crystal structure e functional analysis of lipoamide dehydrogenase from *Mycobacterium tuberculosis*. *J. Biol. Chem. 280*, 33977–33383.
5. Wood, Z. A., Poole, L. B., and P. Karplus, P. A. (2001) Structure of intact AhpF reveals a mirrored thioredoxin-like active site and implies large domain rotations during catalysis. *Biochemistry 40*, 3900–3911.
6. Waksman, G., Krishna, T. S. R., Williams, C. H., Jr., and Kuriyan, J. (1994) Crystal structure of *Escherichia coli* thioredoxin reductase refined at 2 Å resolution. Implications for a large conformational change during catalysis. *J. Mol. Biol. 236*, 800–816.
7. Yoshida, T., Oka, S., Masutani, H., Nakamura, H., and Yodoi, J. (2003) The role of thioredoxin in the aging process: Involvement of oxidative stress. *Antioxid. Redox Signaling 5*, 563–570.
8. Akif, M., Suhre, K., Verma, K., and Mande, S. C. (2005) Conformational flexibility of *Mycobacterium tuberculosis* thioredoxin reductase: Crystal structure and normal mode analysis. *Acta Crystallogr. D61*, 1603–1601.
9. Bjornstedt, M., Hamberg, M., Kumar, S., Xue, J., and Holmgren, A. (1995) Human thioredoxin reductase directly reduces lipid hydroperoxides by NADPH and selenocystine strongly stimulates the reaction via catalytically generated selenols. *J. Biol. Chem. 270*, 11761–11764.
10. Arnér, E. S. J., Zhong, L., and Holmgren, A. (1999) Preparation and assay of mammalian thioredoxin and thioredoxin reductase. *Methods Enzymol. 300*, 226–239.
11. Kuriyan, J., Krishna, T. S. R., Wong, L., Guenther, B., Pahler, A., Williams, C. H., Jr., and Model, P. (1991) Convergent evolution of similar function in two structurally divergent enzymes. *Nature 352*, 172–174.
12. Dai, S., Saarinen, M., Ramaswamy, S., Meyer, Y., Jacquot, J. P., and Eklund, H. (1996) Crystal structure of *Arabidopsis thaliana* NADPH dependent thioredoxin reductase at 2.5 Å resolution. *J. Mol. Biol. 264*, 1044–1057.
13. Lennon, B. W., Williams, C. H., Jr., and Ludwig, M. L. (2000) Twists in catalysis: Alternating conformations of *Escherichia coli* thioredoxin reductase. *Science 289*, 1190–1194.
14. Giaever, G.; et al. (2002) Functional profiling of the *Saccharomyces cerevisiae* genome. *Nature 418*, 387–391.
15. Arnér, E. S., and Holmgren, A. (2000) Physiological functions of thioredoxin and thioredoxin reductase. *Eur. J. Biochem. 267*, 6102–6109.
16. Laskowski, R. A., MacArthur, M. W., Moss, D. S., and Thornton, J. M. (1993) PROCHECK: a program to check the stereochemical quality of protein structures. *J. Appl. Crystallogr. 26*, 283–291.
17. Ruggiero, A., Masullo, M., Ruocco, M. R., Grimaldi, P., Lanzotti, M. A., Arcari, P., Zagari, A., and Vitagliano, L. (2009) Structure and stability of a thioredoxin reductase from *Sulfolobus solfataricus*: A thermostable protein with two functions. *Biochim. Biophys. Acta 1794*, 554–562.
18. Krissinel, E., and Henrick, K. (2004). Secondary-structure matching (SSM), a new tool for fast protein structure alignment in three dimensions. *Acta Cryst. D60*, 2256−2268.
19. Schultz, G. E. (1980) Gene duplication in glutathione reductase. *J. Mol. Biol. 138*, 135–147.
20. Krissinel, E., and Henrick, K. (2007) Inference of macromolecular assemblies from crystalline state. *J. Mol. Biol. 372*, 774–797.
21. Amorim, G. C., Pinheiro, A. S., Netto, L. E. S., Valente, A. P., and Almeida, F. C. M. (2007) NMR solution structure of the reduced form of thioredoxin 2 from *Saccharomyces cerevisiae*. *J. Biomol. NMR 38*, 99–104.
22. Pinheiro, A. S., Amorim, G. C., Netto, L. E., Almeida, F. C., and Valente, A. P. (2008) NMR solution structure of the reduced form of thioredoxin 1 from *Sacharomyces cerevisiae*. *Proteins 70*, 584–587.
23. Negri, A., Rodríguez-Larrea, D., Marco, E., Jiménez-Ruiz, A., Sánchez-Ruiz, J. M., and Gago, F. (2009) Protein-protein interactions at an enzyme-substrate interface: Characterization of transient reaction intermediates throughout a full catalytic cycle of *Escherichia coli* thioredoxin reductase. *Proteins 78*, 36–51.
24. Mulrooney, S. B., and Williams, C. H., Jr. (1994) Potential active-site base of thioredoxin reductase from *Escherichia coli*: examination of histidine245 and aspartate139 by site-directed mutagenesis. *Biochemistry 22*, 3148–3154.
25. Kirkensgaard, K. G., Hägglund, P., Finnie, C., Svensson, B., and Henriksen, A. (2009) Structure of *Hordeum vulgare* NADPH-dependent thioredoxin reductase 2. Unwinding the reaction mechanism. *Acta Crystallogr. D65*, 932–941.
26. Vignols, F., Bréhélin, C., Surdin-Kerjan, Y., Thomas, D., and Meyer, Y. (2005) A yeast two-hybrid knockout strain to explore thioredoxin-interacting proteins in vivo. *Proc. Natl. Acad. Sci. U.S.A. 102*, 16729–16734.

27. Bieger, B., and Essen, L. O. (2001) Crystal structure of the catalytic core component of the alkylhydroperoxide reductase AhpF from *Escherichia coli*. *J. Mol. Biol. 307*, 1–8.
28. Poole, L. B. (2005) Bacterial defenses against oxidants: Mechanistic features of cysteine-based peroxidases and their flavoprotein reductases. *Arch. Biochem. Biophys. 433*, 240–254.
29. Wieles, B., van Noort, J., Drijfhout, J. W., Offringa, R., Holmgren, A., and Ottenhoff, T. H. M. (1995) Purification and functional analysis of the *Mycobacterium leprae* thioredoxin/thioredoxin reductase hybrid protein. *J. Biol. Chem. 270*, 25604–25606.
30. Wieles, B., Soolingen, D., Holmgren, A., Offringa, R., Ottenhoff, T., and Thole, J. (1995) Unique gene organization of thioredoxin and thioredoxin reductase in *Mycobacterium leprae*. *Mol. Microbiol. 16*, 921–929.
31. Biterova, E. I., Turanov, A. A., Gladyshev, V. N., and Barycki, J. J. (2005) Crystal structures of oxidized and reduced mitochondrial thioredoxin reductase provide molecular details of the reaction mechanism. *Proc. Natl. Acad. Sci. U.S.A. 102*, 15018–15023.
32. Sandalova, T., Zhong, L., Lindqvist, Y., Holmgren, A., and Schneider, G. (2000) Three-dimensional structure of a mammalian thioredoxin reductase: Implications for mechanism and evolution of a selenocysteine-dependent enzyme. *Proc. Natl. Acad. Sci. U.S.A. 98*, 9533–9538.
33. Angelucci, F., Sayed, A. A., Williams, D. L., Boumis, G., Brunori, M., Dimastrogiovanni, D., Miele, A. E., Pauly, F., and Bellelli, A. (2009) Inhibition of *Schistosoma mansoni* thioredoxin glutathione reductase by auranofin: Structural and kinetic aspects. *J. Biol. Chem. 284*, 28977–28985.
34. Su, D., and Gladyshev, V. N. (2004) Alternative splicing involving the thioredoxin reductase module in mammals: A glutaredoxin-containing thioredoxin reductase 1. *Biochemistry 43*, 12177–12188.
35. Pedrajas, J. R., Kosmidou, E., Miranda-Vizuete, A., Gustafsson, J. A., Wright, A. P., and Spyrou, G. (1999) Identification and functional characterization of a novel mitochondrial thioredoxin system in *Saccharomyces cerevisiae*. *J. Biol. Chem. 274*, 6366–6373.
36. Holmgren, A., and Björnstedt, M. (1995) Thioredoxin and thioredoxin reductase. *Methods Enzymol. 252*, 199–208.
37. Martí, M. C., Olmos, E., Calvete, J. J., Díaz, I., Barranco-Medina, S., Whelan, J., Lázaro, J. J., Sevilla, F., and Jiménez, A. (2009) Mitochondrial and nuclear localization of a novel pea thioredoxin: Identification of its mitochondrial target proteins. *Plant Physiol. 150*, 646–657.
38. Sotirchos, I. M., Hudson., A. L., Ellis, J., and Davey, M. W. (2009) A unique thioredoxin of the parasitic nematode *Haemonchus contortus* with glutaredoxin activity. *Free Radical Biol. Med. 46*, 579–585.
39. Oliveira, M. A., Netto, L. E. S., Medrano, F. J., Barbosa, J. A., Alves, S. V., and Guimarães, B. G. (2005) Crystallization and preliminary X-ray diffraction analysis of NADPH-dependent thioredoxin reductase I from *Saccharomyces cerevisiae*. *Acta Crystallogr. F61*, 387–390.
40. Navaza, J. (1994) AmoRe: An automated package for molecular replacement. *Acta Crystallogr. D57*, 1367–1372.
41. Murshudov, G. N., Vagin, A. A., and Dodson, E. J. (1997) Refinement of macromolecular structures by the maximum-likelihood method. *Acta Crystallogr. D53*, 240–255.
42. Jones, T., Zou, J., Cowan, S., and Kjeldgaard, M. (1991) Improved methods for binding protein models in electron density maps and the location of errors in these models. *Acta Crystallogr. A47*, 110–119.
43. Perrakis, A., Sixma, T. K., Wilson, K. S., and Lamzin, V. S. (1997) wARP: Improvement and extension of crystallographic phases by weighted averaging of multiple refined dummy atomic models. *Acta Crystallogr. D53*, 448–455.
44. Winn, M. D., Isupov, M. N., and Murshudov, G. N. (2001) Use of TLS parameters to model anisotropic displacements in macromolecular refinement. *Acta Crystallogr. D57*, 122–133.
45. Thompson, J. D., Gibson, T. J., Plewniak, F., Jeanmougin, F., and Higgins, D. G. (1997) The CLUSTAL_X windows interface: Flexible strategies for multiple sequence alignment aided by quality analysis tools. *Nucleic Acids Res. 25*, 4876–4882.
46. Livingstone, C. D., and Barton, G. J. (1993) Protein sequence alignments: A strategy for the hierarchical analysis of residue conservation. *Comput. Appl. Biosci. 9*, 745–756.
47. Clamp, M., Cuff, J., Searle, S. M., and Barton, G. J. (2004) The Jalview Java alignment editor. *Bioinformatics 20*, 426–427.
48. Holm, L., and Sander, C. (1993) Protein structure comparison by alignment of distance matrices. *J. Mol. Biol. 233*, 123–138.
49. Gibrat, J. F., Madej, T., and Bryant, S. H. (1996) Surprising similarities in structure comparison. *Curr. Opin. Struct. Biol. 3*, 377–385.
50. Collaborative Computational Project, Number 4 (1994) The CCP4 suite: Programs for protein crystallography. *Acta Crystallogr. D50*, 760–763.
51. Emsley, P., and Cowtan, K. (2004) Coot: Model-building tools for molecular graphics. *Acta Crystallogr. D20*, 2126–2132.
52. Landau, M., Mayrose, I., Rosenberg, Y., Glaser, F., Martz, E., Pupko, T., and Ben-Tal, N. (2005) ConSurf 2005: The projection of evolutionary conservation scores of residues on protein structures. *Nucleic Acids Res. 33*, W299–W302.
53. Zhang, Z., Bao, R., Zhang, Y., Yu, J., Zhou, C. Z., and Chen, Y. (2009) Crystal structure of *Saccharomyces cerevisiae* cytoplasmic thioredoxin reductase Trr1 reveals the structural basis for species-specific recognition of thioredoxin. *Biochim. Biophys. Acta 1794*, 124–128.